A systematic approach to the determination of SRAF capabilities in high end mask manufacturing

Christian Bürgel, Martin Sczyrba, G.R. Cantrell
AMTC Dresden, Rähnitzer Allee 9, 01109 Dresden, Germany

ABSTRACT

The continued shrink of integrated circuit patterns increases the demand for reticle enhancement techniques (RET). The application of Sub Resolution Assist Features (SRAFs) is pushing mask processes to the resolution limit. Many Chemically Amplified Resists (CAR) used in current photomask processes do not have the capability to fully meet the current demand for SRAF resolution.

Often the resulting quality of small SRAFs suffers from pattern fidelity limitations like Line End Shorting (LES) and corner rounding. While small SRAFs might physically resolve on the mask, these limitations cause massive nuisance detections at defect inspections. In a productive environment, high levels of nuisance detections are not acceptable due to the cycle time impact from classification and review.

The AMTC systematically investigated the SRAF capability of different mask processes in order to better understand the process limitations as well as to predict the manufacturability of customer patterns. This investigation uses high sensitivity inspections of a specially designed test pattern to determine the SRAF capability limits. An overview of the predicted SRAF capabilities for different resists and blank substrates is provided along with verification on customer layouts.

Keywords: Reticle Enhancement Techniques (RET), Sub Resolution Assist Features (SRAFs), Line End Shorting (LES), Chemically Amplified Resist (CAR), inspection

1. INTRODUCTION

The continued shrink of circuit patterns towards 22nm and 20nm design rules places aggressive SRAF demands on photomask manufacturers. SRAF sizes and lengths are shrinking, in addition to customers demanding both opaque and clear SRAF tones on the same mask.[1] Often mask processes are incapable of meeting such customer requirements with SRAF limitations ranging from completely unresolved patterns, to collapsed opaque or unopened clear SRAFs, to reduced pattern fidelity and stability of small SRAFs, driven mostly by LES and corner rounding effects.

Usually there is little to no room for mask processes to improve SRAF resolution and stability since it is almost entirely determined by the CAR characteristics. Typically, only the application of special lithographic conditions can improve SRAF capability, but even under these circumstances the improvement is rather limited.[2] Even mask processes capable of resolving small SRAFs often suffer from massive SRAF nuisance detections during final inspections.

In the past photomask manufacturers circumvented high numbers of nuisance detections by a selective de-sense of the inspection system for the SRAF patterns, such as Thin Line De-sense (TLD) on KLA systems, and Variable Sensitivity Detection (VSD) on NuFlare systems.[3,4,5,6] However with shrinking SRAF sizes and smaller distances to main patterns, the effect of the SRAFs on printed CDs becomes more and more pronounced.[7] For this reason and the risk of missing critical defects, customers might no longer accept a mask with selective de-sense inspection leaving the mask maker with the problem of massive nuisance detections.

In order to precisely predict the SRAF capability in a productive environment, the AMTC has designed a special SRAF test pattern and inspected this pattern using high sensitivity settings already in development for new mask processes. This new test pattern allows SRAF characterization by a systematic variation of SRAF size, length *and* its environment, rather than using simple test patterns [8,9] or outdated customer pattern cut outs. High sensitivity inspections of this new SRAF pattern facilitate adequate predictions of customer pattern performance for new design rules, even at early stages in process development.

2. EXPERIMENTAL

2.1 Layout of the SRAF Cell

AMTC's newly designed SRAF test pattern consists of a series of specially designed SRAF test cells. Within each test cell the SRAF CD (width) is fixed, but the length of the SRAF is varied from 50µm down to sub 500nm. This design addresses the topic of variable SRAF lengths often required on customer layouts. As a second variable, the writing density (WD) around the SRAF is varied to simulate the variation in pattern densities for different kind of masks, *e.g*, contact and VIA, metal, and gate/active layers. The SRAF test cell contains simple straight SRAFs as well as complex, angled SRAFs with all four corner types to identify systematic issues with these shapes. The size of a single SRAF test cell is large enough so that the number of SRAFs in each cell ranges from ~200,000 to ~1 Million, depending upon the writing density.

These newly designed SRAF test cells were incorporated into a standard test mask pattern used to test Critical Dimension (CD) capability of current processes. This approach couples SRAF characterization with a routine CD check to verify results are within the normal process capability and not an atypical event. SRAF test cells were arranged on this standard test pattern in a multi die configuration to allow characterization via inspections as a function of SRAF size, length, WD and shape. Finally, these SRAF test cells were placed on this standard test pattern in reverse tone, allowing characterization of clear and opaque SRAFs on the same mask.

2.2 Inspection setup and data analysis

A high end inspection system from NuFlare Technology ® (NPI-5000+) was utilized for SRAF characterization. This tool inspects with a 199nm light in transmitted and reflected modes simultaneously. The SRAF test masks were inspected in Die-to-Die (D2D) as well as in Die-to-DataBase (D2DB) mode in order to qualitatively compare the minimum SRAF size results. The selected defect size was 0.035µm but in the case of massive detections, a relaxation to 0.040µm was allowed.

A set of SRAF test masks using different CARs and blank substrates (advanced PSM versus advanced Binary on MoSi (BIM)) were manufactured and inspected to compare the capability of mature and state of the art CARs for 50keV exposure. Table 1 gives an overview of this SRAF test mask set.

Table 1. Overview of resist, blank types and inspection modes used for SRAF characterization

	Blank Type	
Resist	**BIM**	**PSM**
advanced pCAR	D2D/D2DB	#N/A
mature pCAR	D2D	D2D

For determining SRAF capability limits, plots of SRAF detections versus size for each length/WD combination were prepared. Images of the largest SRAF CD without massive detections were reviewed in detail to separate between normal process related defects and SRAF detections. A single SRAF related detection out of >500,000 SRAFs was ruled as a non complying SRAF for customer layout purposes.

3. RESULTS AND DISCUSSIONS

3.1 Die-to-Die and Die-to-DataBase mode inspections for clear SRAFs on BIM mask using advanced 50kev CAR

After the SRAF test mask was manufactured it was verified via CD measurements to adequately represent the selected process. In addition, single SRAFs for each combination of variables (CD, length, WD, tone, and complexity) were measured on a CD SEM system. A review of the top down CD SEM images was performed to identify the SRAF combinations with a gross failure such as visible interruption, unopened pattern, etc. The areas containing these SRAF failures were excluded from the following inspections.

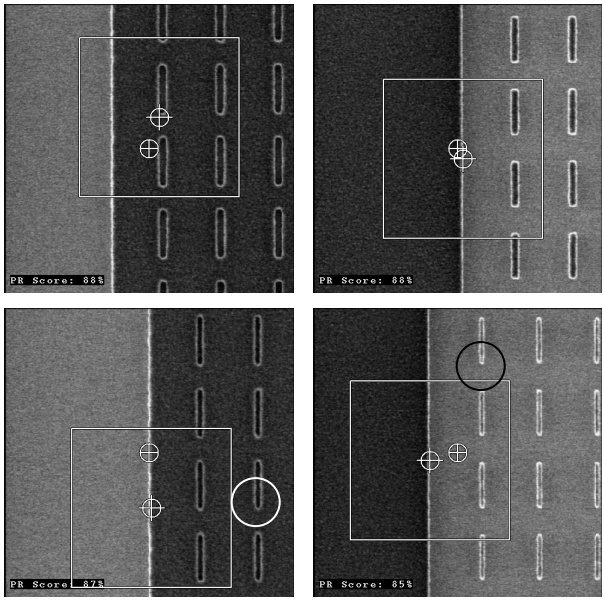

Figure 1. CD SEM top down images of SRAF patterns (Resist on Chrome). The top two images show resolved and stable clear (left) and opaque (right) SRAF patterns, while the two bottom images show SRAFs with LES issues (circled).

After CD verification, the SRAF test mask was inspected on the NuFlare NPI-5000+ system in Die-to-Die and DataBase modes using transmitted and reflected light simultaneously (T&R mode). The SRAF test mask was inspected until completion or until detection overflow was reached. If the CD SEM review indicated areas with potentially good SRAFs, the inspection was restarted to capture these areas. This process was repeated until all SRAF test cells of interest were inspected.

Figure 2 shows a typical inspection result for straight clear SRAFs in Die-to-Die mode at 0.035µm defect size, with the SRAF CD on the x-axis and the number of defect detections on the y-Axis. Every graph contains four lines, each representing a different SRAF length (A to D: long (50µm) to short (<500nm)), while each of the four graphs represents a different writing density. The number of detections increases rapidly at a certain SRAF CD indicating a quality limit for SRAF resolution.

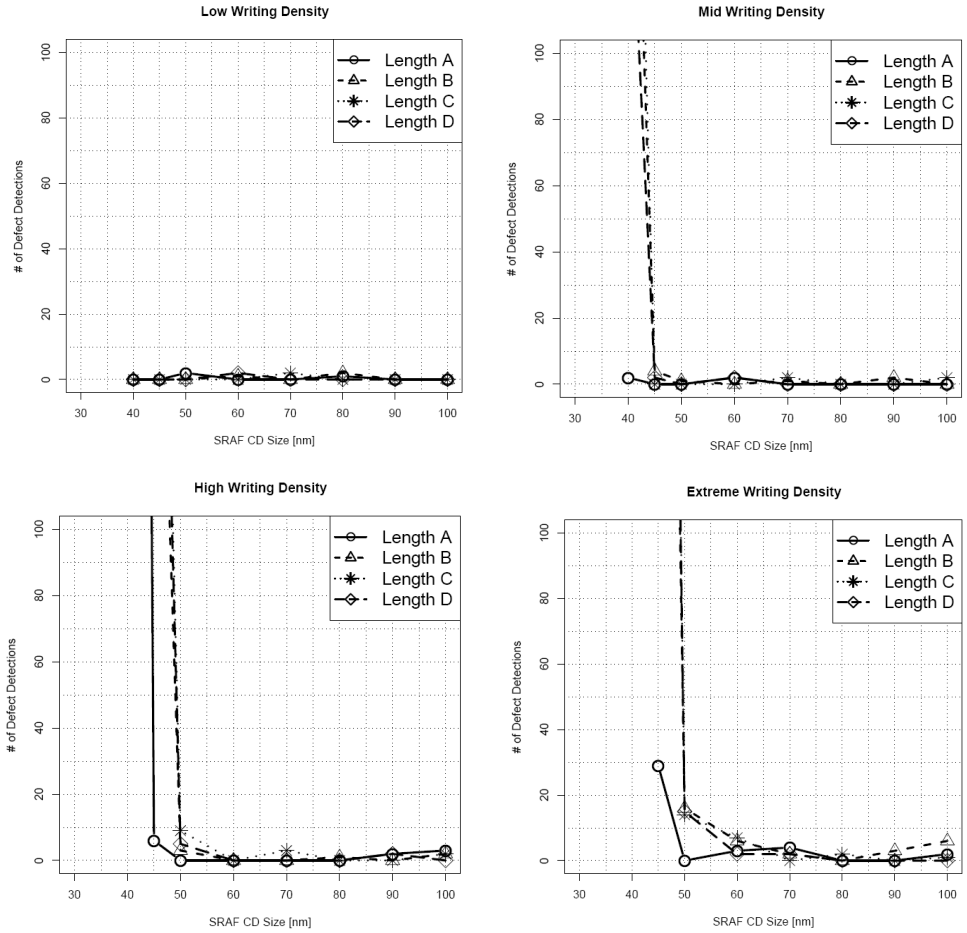

Figure 2. Defect inspection results at 0.035µm defect size (Die-to-Die mode) for the different writing densities and SRAF lengths. The number of defect detections vs. SRAF CD size indicates the quality limit of the SRAF.

Interestingly this quality limit shows hardly any dependency on the SRAF length, since the number of detections for the different SRAF lengths always start to increase at the same CD size (except for the very long SRAFs). In contrast, the quality limit depends heavily on the *writing density*. The process tested in Figure 2 can produce good and stable SRAFs down to 40nm for low writing densities, while it is limited to 60-70nm SRAFs for high and extremely high writing densities. This is an important finding because the achievable SRAFs for a contact mask (low WD) and a gate mask (high WD) are significantly different. This also demonstrates why customer pattern cut outs can not adequately predict the SRAF capability.

One potential reason for this behavior relates to underexposed SRAFs in high writing densities due to a limited Proximity Effect Correction (PEC). While 50keV exposure tools can correct for proximity effects in a range of ~10µm, the tool algorithms can not correct for short range effects at <100nm, which is larger than the targeted SRAF size. As long as the writing density is low, the total dose is sufficient to properly expose the small SRAFs, although the short range proximity effect is not properly corrected. However with an increase in long range writing densities, the dose is continuously reduced by the PEC algorithm making the unaccounted for, short range proximity effect significant. The resulting SRAF dose thus becomes insufficient, leading to imperfectly shaped patterns.

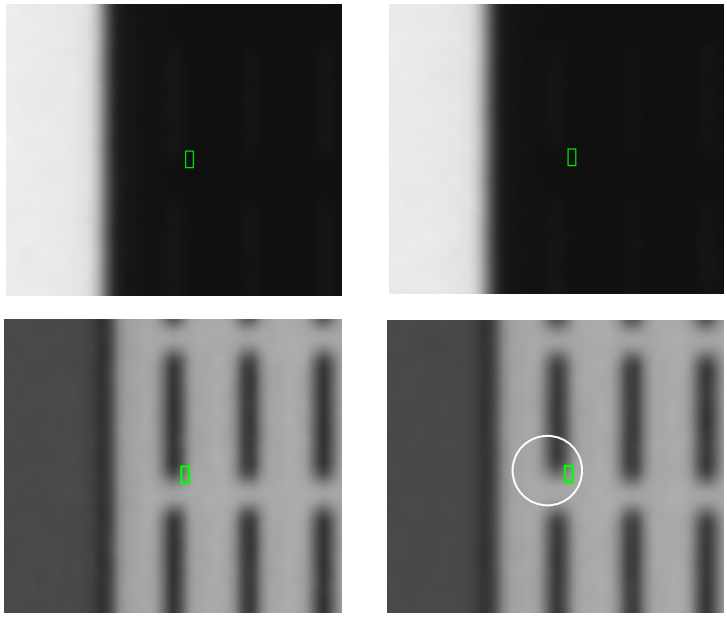

Figure 3. This figure shows the transmitted light (top) and reflected light (bottom) image of the defective (right) and reference die (left). Since the SRAF is too small, the contrast of the transmitted light image is almost collapsed and is of no use for quality assessment. The reflective light picture still images the SRAF with the defective shortened SRAF in the right image (circled).

Figure 3 shows a typical detection of the inspection system on a SRAF affected by increased LES. At very small sizes the contrast of the SRAF image in transmitted light is almost collapsed, resulting in a very low sensitivity of the inspection tool for SRAFs in transmitted light. This effect has already been reported by Yamashita et.al.[6] However, in the reflected light image the SRAF is clearly visible, as well as the line end error. This is a typical signature found in all clear SRAFs defect detections: the reflected light image shows the error. Thus one should consider using reflected light in production environment inspections in order to properly inspect clear SRAFs.

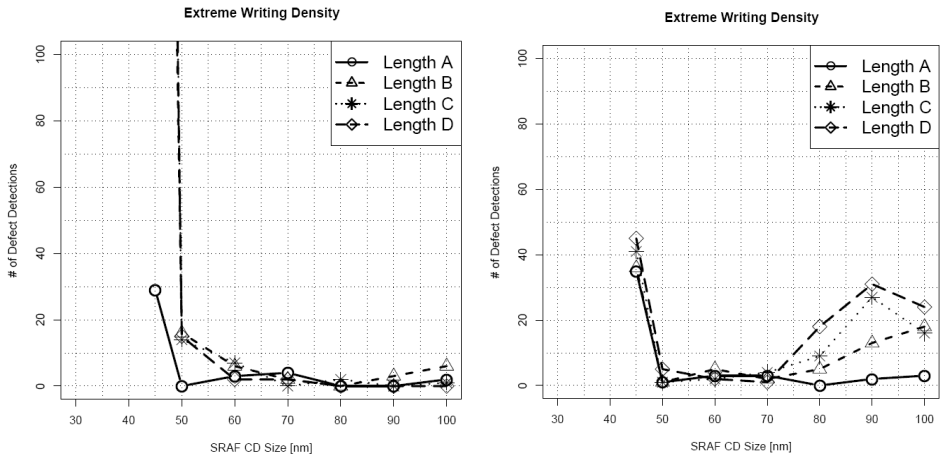

Figure 4. Comparison of the resulting defect detections of Die-to-Die inspections on clear SRAFs for an advanced 50keV CAR resist for straight (left) and angled (right) SRAFs at extremely high WD.

Figure 4 shows the comparison of straight and angled SRAFs for the extreme high writing density. The quality limit for small SRAFs is unchanged, regardless if the process had to build straight or angled SRAFs with tiny corners. However, for larger SRAFs, the angled type shows more defect detections compared to straight SRAFs. A detailed review of inspection images revealed these detections to be located at the SRAF corners. In this case, the instability has been observed in transmitted light images, therefore the number of detections decreases with smaller SRAF sizes due to the

above mentioned collapse of the transmitted light contrast. These defect detections correspond to very little nuisance detections at the SRAF corners and are not detected at 0.04µm defect size and thus do not limit mask production for this targeted defect size.

Clear SRAFs were also inspected in DataBase mode, which confirm the capabilities derived from Die-to-Die inspections as shown in Figure 5. Although a lower number of nuisance detections are observed in DataBase mode inspections, the quality limit remains unchanged, giving the mask maker no resolution gain by the inspection mode selection.

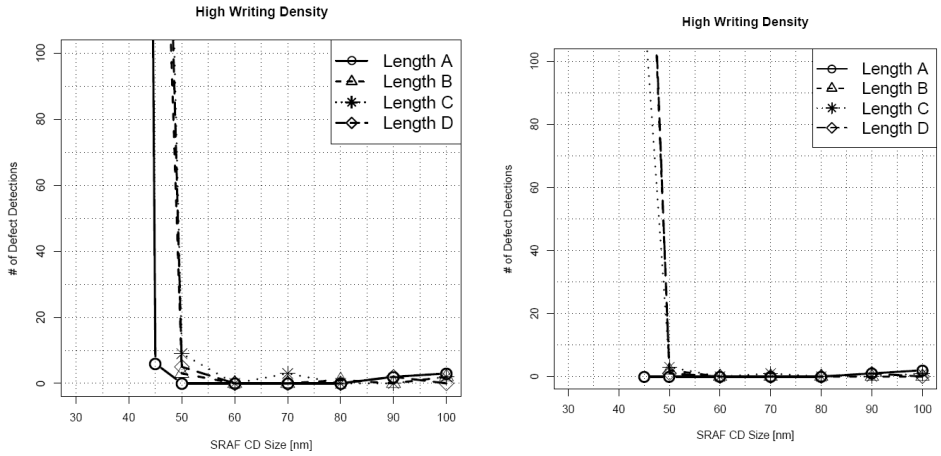

Figure 5. Defect inspection results at 0.035µm defect size for Die-to-Die (left) and DataBase mode (right) for the high writing density and SRAF length. Both inspection modes indicate the same lower quality limit.

Since the SRAF quality limits for both inspection modes were the same, all further results were obtained with Die-to-Die inspections which were easier to set up and consumed less tool time.

The estimated clear SRAF capabilities for masks built with the advanced pCAR process are summarized in Table 2.

Table 2. Estimated clear SRAF capabilities at 0.04µm defect size in Die-to-Die and DataBase modes.

Mask Type	D2D	D2DB
Contact/VIA	40nm	40nm
Metal	50nm	50nm
Gate/Active	60nm	60nm

3.2 Die-to-Die mode inspections for opaque SRAFs on BIM mask using advanced 50kev CAR

Figure 6 shows Die-to-Die inspection results for straight opaque SRAFs. In this case the selected defect size was 0.04µm due to massive LES detections at 0.035µm sensitivity. Similar to the clear SRAFs, the writing density has a major impact on the resulting SRAF capability, while the SRAF length has just a minor impact (except for very long SRAFs).

In contrast to clear SRAFs, the inspection tool detects pattern instabilities of opaque SRAFs (mainly LES issues) in transmitted light images, since the contrast of the reflective light image is poor.[6] Therefore the classical approach of transmitted light inspections is sufficient for assessing the quality of opaque SRAFs.

The estimated opaque SRAF capabilities for masks built with the advanced pCAR process are summarized in Table 3.

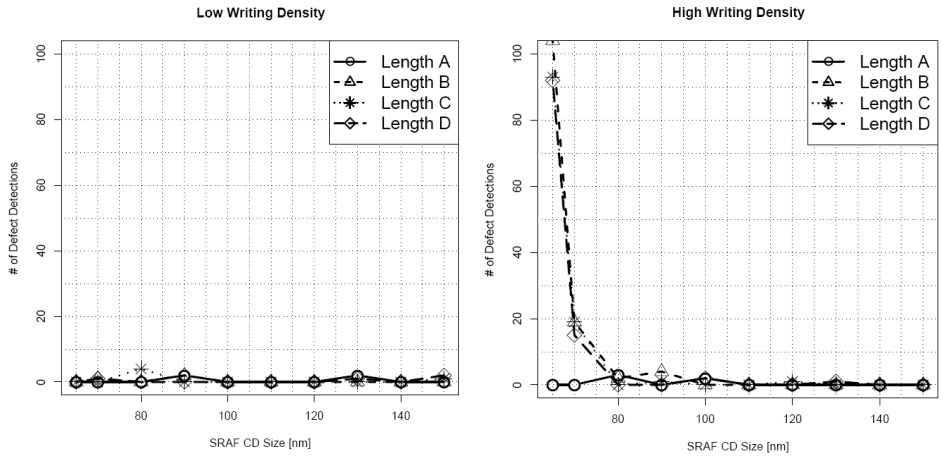

Figure 6. Defect inspection results for straight opaque SRAFs at 0.04µm defect size for two different writing density examples and SRAF length. The number of defect detections vs. SRAF CD size indicates the quality limit of the SRAF.

Table 3. Estimated opaque SRAF capabilities at 0.04µm defect size.

Mask Type	D2D
Metal	70nm
Gate/Active	80nm

3.3 Impact of selected Defect size on capability of opaque SRAFs

According to Table 3, the resulting capability for opaque SRAFs at a defect size of 0.04µm is not meeting the demand of ~60-65nm as predicted by ITRS.[1] A detailed analysis of the defect detections showed the estimated difference between reference and test image was only slightly above the threshold value of the corresponding detector(s). This indicates a better capability can be achieved with a slight relaxation of the defect size which effects threshold value changes in the inspection system.

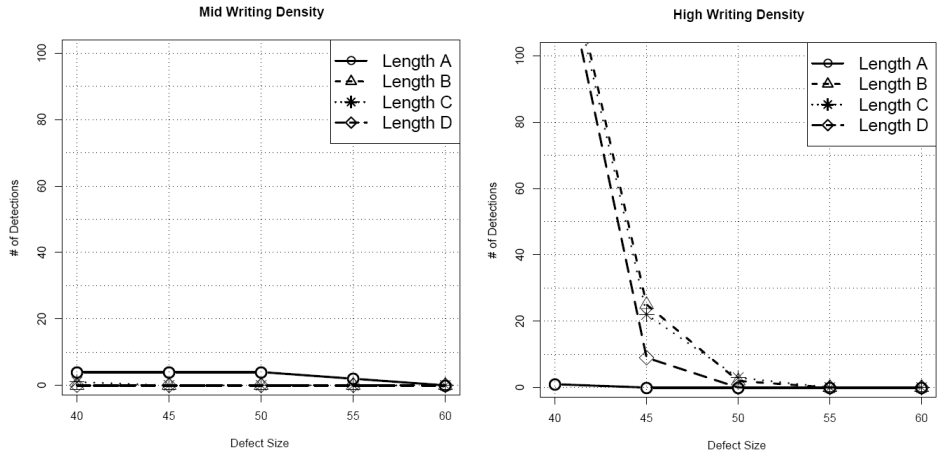

Figure 7. Defect inspection results for 65nm opaque SRAFs at various defect sizes for the two writing densities and SRAF length. The number of defect detections vs. SRAF CD size indicates the quality limit of the SRAF.

The test mask was re-inspected at different defect sizes, where the threshold value was adjusted stepwise to meet sensitivity settings of 0.045µm, 0.05µm, 0.055µm and 0.06µm respectively. Since all opaque SRAFs of 80nm and larger

already passed at 0.04µm defect size, the focus was changed to 65nm SRAFs where the process was estimated to be incapable.

Figure 7 depicts the results of the de-sense test on opaque SRAFs. As expected the number of detections decreases with the increased relaxation of the sensitivity settings. However, a significant change of 15nm in defect size is needed to gain full capability for 65nm opaque SRAFs for the higher writing density.

Table 4. Estimated final SRAF capability for opaque SRAFs at different defect sizes in Die-to-Die mode.

Mask Type	**Inspection Sensitivity**			
	0.04µm	**0.045µm**	**0.05µm**	**0.055µm**
Metal	70nm	65nm	65nm	65nm
Gate/Active	80nm	75nm	70nm	65nm

3.4 Comparison of advanced vs. mature pCAR on BIM

A second SRAF test mask was manufactured using a mature pCAR for 50keV exposure. This mask was inspected identically to the advanced pCAR except 0.04µm defect size was used due to thousand of nuisance detections (even on non SRAF patterns) at 0.035µm.

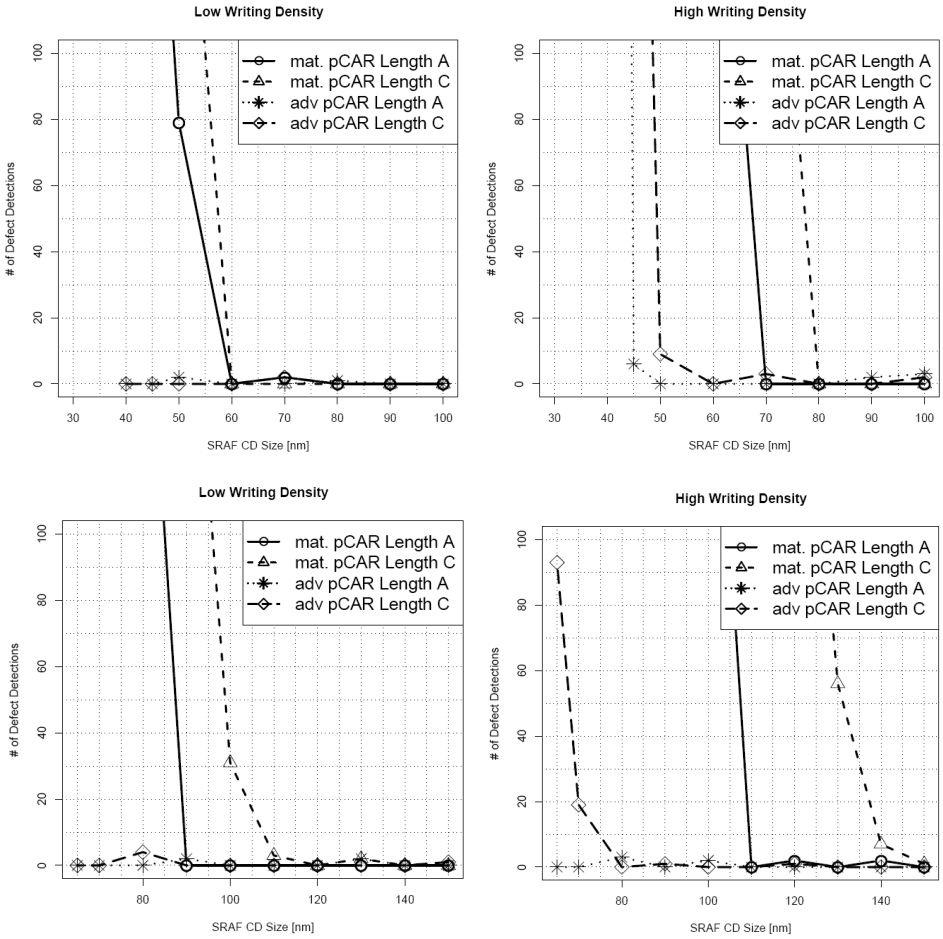

Figure 8. Comparison of the resulting defect detections of Die-to-Die inspections on clear (top) and opaque (bottom) SRAFs for an advanced and mature 50keV CAR resist for low and high writing density.

Figure 8 illustrates the advanced resist has a 20-30nm advantage in clear SRAF resolution and about 45-50nm for opaque SRAFs compared to the mature pCAR. In addition, the same writing density effect on SRAF capability limits is observed with the mature pCAR, which lends further evidence to the notion of PEC correction as a potential root cause for this phenomenon.

3.5 Comparison of PSM vs. BIM for mature pCAR

A third SRAF mask was built and analyzed using the mature pCAR on an advanced PSM blank and compared to the results obtained with the BIM blank. Figure 9 shows that there is no difference in SRAF capability between the BIM and PSM blanks for the mature pCAR. This is a strong indication that the final resolution is determined by the pCAR and not by the etch process, assuming similar etch biases. As for BIM, the writing density impact on SRAF capabilities can be seen for the PSM blank as well, assuming there are no etch process effects.

Since the etch bias for a PSM mask is usually higher, the PSM process might resolve a smaller opaque SRAF than the BIM process. Assuming the same CD targeting in resist for both blank types, the higher etch bias for PSM requires a larger data bias, making opaque SRAF larger resulting in a better capability. However, larger data biases make clear SRAFs smaller, giving the lower etch bias BIM process slight advantages.

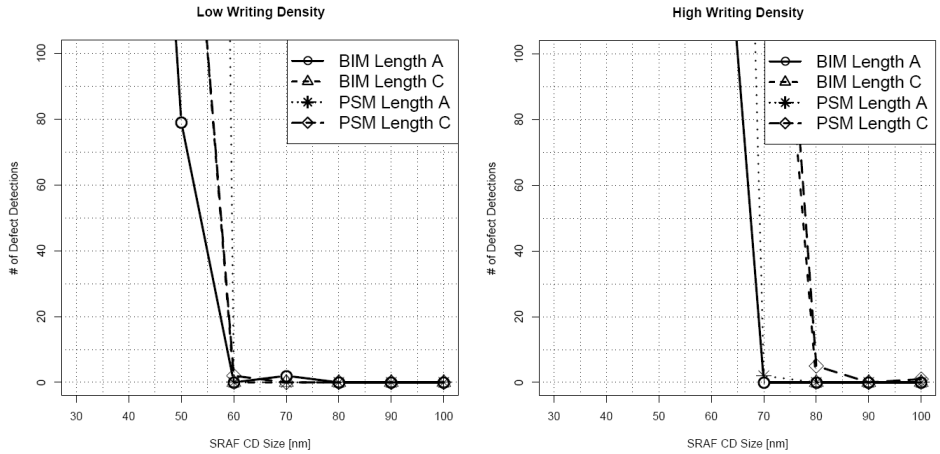

Figure 9. Comparison of the resulting defect detections of Die-to-Die inspections on clear SRAFs for a mature 50keV pCAR on PSM and BIM blanks for low and high writing densities.

Comparing these results to those of the advanced pCAR (Tables 2 & 3) shows clearly the resist of choice for SRAF requirements of a given product and blank material.

Table 5. Estimated clear and opaque SRAF capabilities at 0.04µm defect size for the mature 50keV pCAR.

Mask Type	Clear SRAF	Opaque SRAF
Contact/VIA	60 nm	N/A
Metal	70nm	120nm
Gate/Active	80nm	150nm

3.6 Comparison of SRAF prediction vs. production results

In order to verify the accuracy of these clear SRAF capabilities, the AMTC created a special SRAF test chip with clear SRAFs smaller than 80nm. This SRAF test chip was placed in two locations on a 32nm design rule reticle with a high writing density and inspected in Die-to-Die mode on the NPI5000+ at 0.04µm defect size. The SRAFs were selectively shrunk to 55nm to challenge the advanced pCAR 50keV process. This special test mask was inspected without problems thus verifying the predicted capability of ~60nm for clear SRAFs on a high load pattern (see Figure 10).

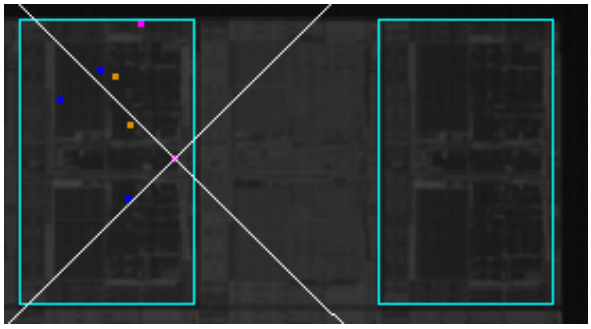

Figure 10. Die-to-Die inspection result of the high load pattern featuring 55nm clear SRAFs. Only a few detections in the test dies were observed.

The special SRAF test chip was placed in reverse tone on the same 32nm design rule reticle with high writing density to verify the opaque SRAF capability. Opaque SRAFs were selectively shrunk to 80nm and at 0.04µm defect size the inspection ran without any problems thus verifying the predicted capability (see Figure 11).

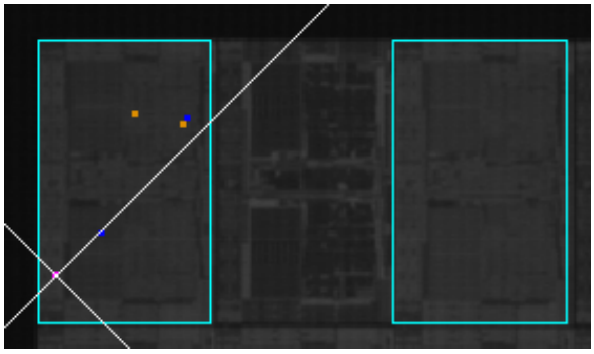

Figure 11. Die-to-Die inspection result of a high load customer pattern featuring 80nm opaque SRAFs. Only a few detections in the test dies were observed.

Finally, the prediction for mature pCAR opaque SRAFs could be verified with several production plates of low and high writing densities. While clear SRAFs on a low writing density mask did not show any issues, opaque SRAFs < 95nm were below the 100% capability prediction. The inspection regularly triggered up to 100 nuisance detections on the line end of these opaque SRAFs (Figure 12). This did not directly verify the mature pCAR opaque SRAF capabilities, but demonstrates that SRAFs of this size are indeed beyond the predicted capability.

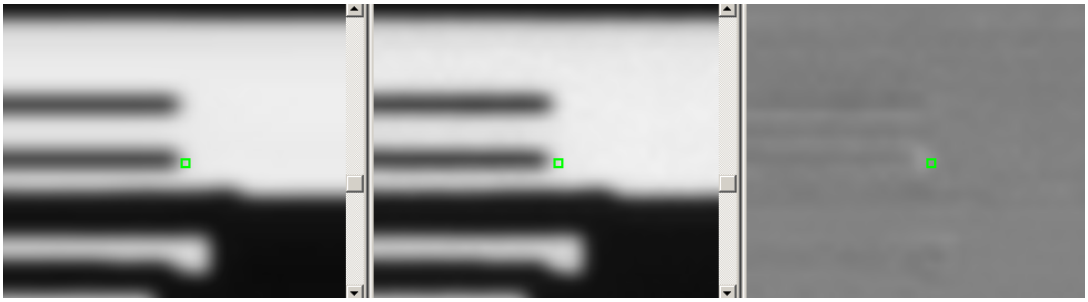

Figure 12. A typical LES defect detection on an opaque SRAF for the mature pCAR (left reference image, center defect image, right difference image) taken from a recent production plate built with the mature pCAR. It can be seen that the inner SRAF is shortened and therefore causing a defect trigger.

4. CONCLUSIONS

In order to address historical gaps between SRAF capability predictions and final capabilities achieved on production masks, the AMTC has designed a new test mask containing SRAF cells with a systematic variation of SRAF CD, length,

writing density, tone, and shape. By using a high end inspection system, a detailed prediction of the SRAF capability for production masks could be derived. Verifications of these SRAF predictions with selected test or production masks containing SRAFs in typical customer layouts were successfully demonstrated.

The AMTC observed a strong impact of writing density (*e.g.*, mask layer) on the resulting SRAF capability, making it impossible to state a single SRAF capability for the entire process. This finding also explains why single clips taken from customer patterns were not capable to fully predict the SRAF capability.

Another important outcome of these experiments is the insensitivity of the inspection tool for clear SRAFs in transmitted light inspections. As a result, a reflective light inspection must be performed at least once during the mask manufacturing process in order to verify the compliance of small clear SRAFs with customer demands.

The powerful utility of this new SRAF test pattern has allowed the AMTC to initiate SRAF capability checks as early as possible in new process developments. This avoids time and cost intensive reworks to address unexpected SRAF limitations and at the same time ensures a robust and predictable process is achieved in a timely manner.

As a next step, the estimation of negative tone SRAF capabilities with a comparison to the available pCAR data is planned. Writing density effects in the negative tone need to be verified since the mechanisms of pattern failure might be different from pCAR (*e.g.*, opaque SRAFs built on nCARs tend to collapse rather than suffer from LES or line edge roughness). Furthermore, an investigation of ultra-short SRAF resolution capabilities (length $\leq$100nm) should be started in order to derive a proper prediction for such highly aggressive SRAF patterns which may be required by mask customers.

ACKNOWLEDGEMENT

AMTC is a joint venture of GLOBALFOUNDRIES and Toppan Photomasks, and gratefully acknowledges the financial support by the German Federal Ministry of Education and Research BMBF under contract numbers 13N9675 (ANTARES).

REFERENCES

[1] ITRS, “Lithography, Optical Mask Requirements, Table LITH5A, 2009”
[2] Kindt, L., Gallagher, E., Levin, J., Kodera, Y., Okawa, Y., Sasaki, Y., “Damage Mechanism and Process optimization for Photomasks with Sub-Resolution Assist Features,” Proc. SPIE 7122, 71220I (2008)
[3] Chen, C., Kim, D., Park, K., Kim, N, Han, S. H., Park, J. H. Chung, D. H., “Improving Inspectability with KLA-Tencor TeraScan thin line de-sense,” Proc. SPIE 6730, 37303O (2007)
[4] Han, S. H., Park, J.H., Chung, D. H., Woo, S. G., Cho, H. K., Kim, D. Chen, C., Park, K. Inderhees, G., ”A pragmatic approach to high sensitivity defect inspection on the presence of mask process variability,“ Proc. SPIE 6730, 373024 (2007)
[5] Goonesekera, A., Lee, I., Mu, B., Dayal, A., “Thin-Line De-sense capability for DataBase mode inspections with KLA-Tencor TeraScanHR,” Proc. SPIE 7028, 70282J (2008)
[6] Yamashita, K., Harabe, N., Hirono, M., Tamura, Y., Isomura, I., Tsuji, Y., Matsumoto, E., “Variable sensitivity detection (VSD) technology for screening SRAF nuisance defects,” Proc. SPIE 7379, 737929 (2009)
[7] Byung-Sung, K., Lee, S., Shin, H., Lee, N., “Size tolerance of sub-resolution assist features for sub-50nm node devices,” Proc. SPIE 6520, 652027 (2007)
[8] Lee, G., Dress, P., Chen, S., Dietze, U., “Reduction of Local CD-Linewidth Variations in Resist Develop through Acoustic Streaming,” Proc. SPIE 7488, 748818 (2009)
[9] Hwang, G., Patil, M., Seo, S., Yu, C., Hur, I., Kim, D. H., Shin, C., Jung, S., Lee, Y., Choi, S., “Patterning Capability and Limitations by Pattern Collapse in 45nm and below Photo Mask Production,” Proc. SPIE 7028, 702824 (2008)